International Journal of Mechanical and Industrial Technology ISSN 2348-7593 (Online)
Vol. 10, Issue 1, pp: (36-52), Month: April 2022 - September 2022, Available at: www.researchpublish.com

Energy and Exergy Analysis of a Copper Oxide Nanoparticle Enhanced Vapour Compression Refrigeration System Using HFC-134a and HFO-1234yf as Refrigerants

K.M, Odunfa[1]; O.A, Opafunso[1], T.A Adeyi[2]

[1]Department of Mechanical Engineering, University of Ibadan, Ibadan, Nigeria

[2]Department of Mechanical Engineering, Lead City University, Ibadan Nigeria

DOI: https://doi.org/10.5281/zenodo.7035062

Published Date: 30-August-2022

Abstract: **Several studies carried out previously showed that the performance analyses of refrigeration systems were investigated based on only the first law of thermodynamics and to calculate the actual loss due to irreversibility in the system, exergy analysis based on second law of thermodynamics is essential. Incorporation of Nano particles in the refrigerants has been observed as a means of reducing irreversibility and improving the performance of Vapour Compression Refrigeration Systems (VCRSs). This study describes a thermal modeling of VCRS where refrigerants HFC-134a and HFO-1234yf are fluids in primary circuit and the copper oxide nanoparticle is the fluid in the secondary circuit. A computational simulation program was used to solve the non-linear equations for the main system components such as compressor, condenser, expansion device and evaporator. It also uses thermophysical properties of HFC-134a, HFO-1234yf and CuO nanoparticle. It's size and the compressor speed to predict the secondary fluids output temperatures, the operating pressures, the compressor power consumption and the system overall energy performance. Results of this study show that the highest improved coefficient of performance is 14.65% in HFC-134a mixed with nanoparticles as compared to the value without nanoparticles. Similarly, it was also observed that second law performance improvement of exergy efficiency range is 11.6% to 12.9% and it's higher in HFC-134a mixture. The reduction in the irreversibility in terms of exergy destruction ratio in the system is 21.4% using the HFC-134a mixture and 18.5% using the HFO-1234yf. Although the mixture of CuO in HFC-134a shows a higher performance in most cases of the system, the HFO-1234yf can be a good replacement for the HFC-134a because of its low GWP and its environmental friendly properties.**

Keywords: **Nano particles, Refrigerants, vapour compression refrigeration system, exergy efficiency, exergy destruction rate.**

Nomenclature

S	Entropy	(kJ/kgK)
Ed	Exergy destruction	(kW)
Ex	Exergy of Refrigerant	(kW)
h	Enthalpy	(kJ/kg)
T	Temperature	(K)
To	Temperature of Dead State	
Tr	Temperature of space	
Tc	Temperature of condenser	
As	surface area of evaporator coil area	(m2)
Cw	water specific heat	(kJ/kg K)
Cp	specific heat	(kJ/kg K
h1-4	enthalpy of refrigerant at different locations of cycle	(kJ/kg)
h	enthalpy of refrigerant at different locations of cycle	(kJ/kg)

hfg	heat transfer coefficient of water	(W/m2 K)
Iev	exergy loss in evaporator	(kJ/kg)
Icomp	exergy loss in compressor	(kJ/kg)
Icond	exergy loss in condenser	kJ/kg)
Icap	exergy loss in capillary tube	(kJ/kg)
K	thermal conductivity	(W/m K)
Mw	mass of water (cooling load)	(kg)
Q	heat flux	(w/m2)
Qc	heat removed from refrigerant	(kJ/kg)
Qe	heat added to refrigerant (refrigeration effect)	(kJ/kg)
s1-4	entropy of refrigerant at different locations of cycle	(kJ/kg)
Ts	surface temperature of evaporator coil	(K)
T∞	average water temperature	(K)
W	compressor work	(kJ/kg)
X'	specific exergy	
D	Diameter	(m)
h	Specific enthalpy	(J/kg)
k	Thermal conductivity	(W/m K)
L	Length	(m)
M	Mass flow rate	(kg/s)
N	Compressor speed	(r.p.m.)
P	Power consumption	(W)
p	Pressure	(Pa)
Q	Volumetric rate of flow	(m3/s)
q	Heat transfer rate	(W)
t	Time	(s)
v	Velocity	(m/s)
x	Refrigerant quality	

Suffixes

air	Environment
avg	Average
b	Brine/nanofluid
C	Compressor
E	Evaporation
i	Inner
in	Input
k	Condensation
L	Liquid
M	Metal
o	Outer
out	Output
r	Refrigerant
sat	Saturated
V	Vapor
w	Water
nf	Nanofluid
m	Base fluid
p	Nanoparticle
ϕ	volume fraction
COP	Coefficient of Performance
WN	with using nanoparticle
WON	without using nanoparticles
L	liquid
g	gas
n	Nanoparticle
o	Oil
r	Refrigerant
n,o	nanoparticle with oil
r,o	refrigerant with oil
r,n,o	refrigerant with nanoparticle and oil
W	Work Rate
EDR	Exergy Destruction Ratio

1. INTRODUCTION

Today, throughout the world several efforts are adopted to reduce energy consumption and saving power for a longer period of time. Larger amount of energy is consumed daily through the use of household gadgets such as general appliances (television, sound systems, fans, lightening, and gadget chargers), heaters, air conditioners and refrigerator. Energy consumption in households via other electrical appliances can be minimized by ensuring that those devices are only switched on whenever they are needed. Contrarily, this method does not work for the refrigeration system since it has to run most of the time [1]. Refrigerators consume significantly high energy and the improvement on their efficiency is essential to minimize greenhouse gas emission [2]. It has been estimated that about 50% of energy consumption in commercial buildings goes to heating, ventilation and air-conditioning (HVAC) systems.[3]. In the face of imminent energy resource crunch there is need for developing thermal systems which are energy efficient, as we know that thermal systems like refrigerators and air conditioners consume large amount of electric power. Therefore, avenues of developing energy efficient refrigeration and air conditioning systems with eco-friendly refrigerants need to be explored. However this area has now been of great interest because of the increase in demand for energy, the cost of conventional fuels, degradation of environment, global warming, depletion of ozone layer and environmental concerns globally. There is urgent need of efficient energy utilization from new and renewable sources of energy for refrigerating system enhancement so as to reduce energy consumption, exergy losses and to increase the rate of cooling [4].To provide the benefits listed above, researchers throughout the previous decades have been proposing, experimenting and testing nanoparticles for the enhancement of refrigerating systems.

Basically, the main purpose of using nanorefrigerant in place of conventional refrigerant in any refrigeration system is to make the design smaller, more compact, lighter, and more efficient. The refrigeration systems working on nanorefrigerants are likely to have its improved cooling capacity. These refrigeration systems consume less power, and hence are more energy efficient. This is due to the fact that nanorefrigerants possess superior thermophysical properties in comparison to the conventional or base refrigerants [5]. Nanoparticle applications have captured the attention of the innovative world due to their special properties and ability to influence the properties of working fluids.[5] Nanofluids are considered as an advanced class of fluids with nanosized particles (1–100 nm) suspended in base fluids.[5,6] Such suspensions form the two-phase system, in which the solid phase is dispersed in the liquid phase [6,7]. Generally, nanoparticles are either metals, nonmetals, or their oxides, which has the ability to improve and influence the conduction and convection thermal performance of the base fluids. [5, 8] Several researchers have observed an enhancement in the thermal conductivity of the base fluid due to the addition of such nanoparticles.[9 – 12] The same results were also observed in the refrigerant-based nanofluids such as, the thermal conductivity enhancement by as much as 104% when carbon nanotube (CNT) nanoparticles are added in R113.[13] The investigation of nanofluids is not limited only to the study of the thermal conductivity; however, many researchers have also studied other thermophysical properties as well such as, viscosity, surface tension, specific heat, etc. It has been observed that the boiling heat transfer is an important area of investigation for refrigerants. The past results published on the boiling heat transfer performance of nanorefrigerants emphasized on its improved performance in comparison to the conventional refrigerants where no nanoparticles were used.

In order to optimize the design of nanoparticles enhanced Vapour Compression Refrigeration systems (VCRs), a thorough energy and exergy analysis of Copper oxide (CuO)/R134a nanofluid to be used to enhance the refrigerating system is required. The analysis will be based on the first law of thermodynamics as used in engineering applications which is concerned only with law of conservation of energy that evaluates Energy analysis; and also the second law of thermodynamics which determines the Exergy analysis that is applied to a system to describe all losses in the system components as well as the whole system. With the use of irreversibility, it is more helpful in determining the optimum operating conditions. However, compared to energy analysis, the exergy analysis can better and accurately show the location of inefficiencies. The exergy method is a relatively new technique in which the basis of evaluation of thermodynamic losses follows the second law rather than the first law of thermodynamics. The results from exergy analysis can be used to assess and optimize the performance of the vapor compression refrigerating systems. And since previous research is more focused on the energy analysis of nanoparticle enhance vapor compression system. Until now, less work is done on the exergy analysis of Nanoparticle Enhance Vapor Compression Systems (NEVCRS).Therefore, in this paper, energy and exergy analysis of a copper oxide NEVCRS using hfc-134a and hfo-1234yf as refrigerants are modelled

2. METHODOLOGY

The figure below shows the operating cycle on a T-S diagram. As shown in the Fig. the standard single stage, saturated vapour compression refrigeration system consists of the following four processes:

Process 1-2: Isentropic compression of saturated vapour in compressor

Process 2-3: Isobaric heat rejection in condenser

Process 3-4: Isenthalpic expansion of saturated liquid in expansion device

Process 4-1: Isobaric heat extraction in the evaporator

In an ideal vapour compression refrigeration cycle, the refrigerant enters the compression at state 1 as saturated vapour and is compressed isentropically to the condenser pressure. The temperature of the refrigerant during this isentropic compression process increases well above the temperature of the surrounding medium. The refrigerant then enters the condenser as superheated vapour at state 2 and leaves as saturated liquid at state 3 as a result of heat rejection to the surroundings. The temperature of the refrigerant at this state is still above the temperature of the surroundings. The saturated liquid refrigerant at state 3 is throttled to the evaporator pressure by passing it through an expansion valve or capillary tube; the temperature of the refrigerant drops below the temperature of the refrigerated space during the process. The refrigerant enters the evaporator at state 4 as a low quality saturated mixture, and it evaporates by absorbing heat from the refrigerated space. The refrigerant leaves the evaporator as saturated vapour and re-enters the compressor, completing the cycle.

Analysis of vapour Compression Refrigeration cycle

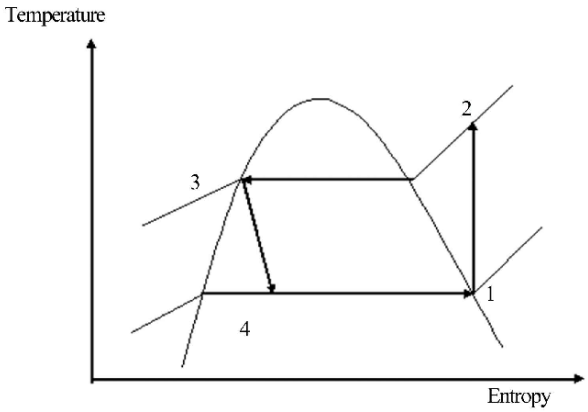

Fig.1: T.S diagram of vapour compression refrigeration system

2.1 Selection of Nanoparticle

The Copper oxide (CuO) nanoparticle is selected to carry out the analysis since less work as been done on its exergetic and irreversibility effects. Copper is a Block D, Period 4 element, while oxygen is a Block P, Period 2 element. Copper oxide nanoparticles appear as a brownish-black powder. They can be reduced to metallic copper when exposed to hydrogen or carbon monoxide under high temperature. They are graded harmful to humans and as dangerous for the environment with adverse effect on aquatic life, also, its key applications whereby it can be used as to improve the homogeneous rate, lower pressure index in the vapor compression refrigerating system, and because of its favorable thermophysical properties which is listed in the table below

Table 1: Properties of Copper oxide

Chemical formula	CuO
CAS No.	1317-38-0
Group	Copper 11 Oxygen 16
Electronic configuration	Copper [Ar] $3d^{10}$ $4s^1$ Oxygen [He] $2s^2$ $2p^4$
Copper content Oxygen content	79.87% 20.10%
Molar mass	79.55 g/mol
Density	6.31 g/cm^3
Melting point	1201°C

Boiling point	2000 °C
Thermal conductivity	32.9W/m.k
Specific heat	
Average Primary Particle size	40nm

2.2 Refrigerant selection

2.2.1: 1,1,1,2-tetrafluoroethane HFC-134a

Also known as, R-134a, Forane 134a, Genetron 134a, Florasol 134a, Suva 134a or, also known as norflurane (INN), is a haloalkane refrigerant with thermodynamic properties similar to R-12 (dichlorodifluoromethane) but with insignificant ozone depletion potential and a somewhat lower global warming potential (1300, compared to R-12's GWP of 2400). It has the formula CH_2FCF_3 and a boiling point of −26.3 °C (−15.34 °F) at atmospheric pressure. R-134a cylinders are colored light blue; Attempts at phasing out its use as a refrigerant with substances that have lower global warming potentials, such as HFO-1234yf are underway. 1,1,1,2-Tetrafluoroethane is a non-flammable gas used primarily as a "high-temperature" refrigerant for domestic refrigeration and automobile air conditioners .Other uses include plastic foam blowing, as a cleaning solvent, a propellant for the delivery of pharmaceuticals (e.g. bronchodilators), wine cork removers, gas dusters and in air driers for removing the moisture from compressed air. 1,1,1,2-Tetrafluoroethane has also been used to cool computers in some over clocking attempts. It is also commonly used as a propellant for air soft air guns. The gas is often mixed with a silicon-based lubricant. Mixtures with air of the gas 1,1,1,2-tetrafluoroethane are not flammable at atmospheric pressure and temperatures up to 100°C (212°F). However, mixtures with high concentrations of air at elevated pressure and/or temperature can be ignited 1,1,1,2-tetrafluoroethane and HFA227ea are propellants of pressurized metered dose inhalers (pMDI) used by asthmatics.

Table 2: Properties of R134a

Chemical formula	CH_2FCF_3
Molar mass	102.03 g/mol
Density	0.00425 g/cm^3, gas
Melting point	−103.3 °C (−153.9 °F; 169.8 K)
Boiling point	−26.3 °C (−15.3 °F; 246.8 K)
Solubility in water	0.15 wt%
Flash point	250 °C (482 °F; 523 K)
Critical temperature ©	252°F or 122°C
Critical pressure (kpa)	588.9 psia (4060.3 kPa [abs])
Specific heat ratio (Cp/Cv)	1.28
ODP	0
GWP (per100 Year)	1200
Safety Group	A1

2.2.2 2,3,3,3-Tetrafluoropropene, or HFO-1234yf

This is a hydrofluoroolefin (HFO) with the formula CH_2=CFCF This colorless gas has been proposed as a replacement for R-134a as a refrigerant in automobile air conditioners. HFO-1234yf is the first in a new class of refrigerants acquiring a global warming potential (GWP) rating one 335th that of R-134a (and only 4 times higher than carbon dioxide, which can also be used as a refrigerant but which has properties significantly different from those of R134a, especially operation at around 5 times higher pressure) and an atmospheric lifetime of about 400 times shorter. HFO-1234yf, which has a 100-year GWP of 4, could be used as a "near drop-in replacement" for R-134a,

Table 3: Properties of HFO-1234yf

Chemical formula	$C_3H_2F_4$
Molar mass	114 g/mol
Density	1.1 g/cm^3 at 25 °C (liquid); 4, air = 1 (gas)
Melting point	−103.3 °C (−153.9 °F; 169.8 K)
Boiling point	−30 °C (−22 °F; 243 K)
Solubility in water	198.2 mg/l at 24 °C, 92/69/EEC, A.6
Vapor pressure	6,067 hPa at 21.1 °C; 14,203 hPa at 54.4 °C

Critical temperature ©	95°C
Pvap, MPa (25°C) Pvap, Mpa (80°C)	0.673 2.47
ODP	0
GWP (per100 Year)	4
Safety Group	A2L

2.3 Performance Analysis

Energy and exergy analyses need some mathematical formulations for the simple vapor compression refrigeration cycle. In the vapor compression system, there are four major components: evaporator, compressor, condenser, and expansion valve. Exergy associated processes [5]. To specify the exergy losses or destructions in the system, thermodynamic analysis losses in various components of the system are not same. A temperature and pressure are denoted by T_0 and P_0, respectively. Exergy is consumed or destroyed due to entropy created depending on this to be made. In this study, the following assumptions are made:

1. Steady state conditions are remained in all the components.
2. Pressure loses in the pipelines are neglected.
3. Heat gains and heat loses from the system or to the system are not considered.
4. Kinetic and potential energy and exergy losses are not considered
5. Degree of subcooling of liquid refrigerant in liquid-vapour heat exchanger (ΔTsub) = 5K.
6. Mechanical efficiency of compressor (η) = 80%.
7. Difference between evaporator and space temperature (Tr – Te) = 20 °C.
8. Evaporator temperature Tevap (in °C) ranging from –40 °C to -10 °C.
9. Condenser temperature Tcond = 40 °C.
10. Dead state temperature (To) = 27 °C.

2.3.1: Mathematical formulation for exergy analysis without Nano

Different components can be arranged in the following ways [6]:

Specific exergy in any state; $\psi = (h - h_o) - T_o(s - s_o)$ (2.1)

For evaporator;

Heat addition in evaporator, $Q = m\,(h1 - h4)$ (2.2)

Exergy destruction, $Iev = m\,(\psi 4 - \psi 1) + Q\,(1 - \frac{T_o}{Tev})$ (2.3)

$$Iev = m\,[(h4 - h1) + T_o\,(s4 - s1)] + Q\,(1 - \frac{T_o}{Tev}) \quad (2.4)$$

For compressor;

Compressor work, $Wc = m(h2 - h1)$ (2.5)

For non – isentropic compression, $hc = \frac{h2s - h2}{\eta c}$ (2.6)

Electrical power, $Wel = \frac{Wc}{\eta mech\ X\ \eta el}$ (2.7)

So, exergy loss, $I_{comp} = m(\psi_1 - \psi_2) + W_{el} = m[(h_1 - h_2) - T_0(s_1 - s_2)] + W_{el}$ (2.8)

For condenser;

$$Q_{cond} = m(h_2 - h_3) \quad (2.9)$$

Exergy loss,

$$I_{cond} = m(\psi_1 - \psi_2) - Q_{cond}\left(1 - \frac{T_s}{T_{cond}}\right) - m(h_2 - h_4) - T_0(s_2 - s_3) - Q_{cond}\left(1 - \frac{T_s}{T_{cond}}\right) \quad (2.10)$$

For expansion valve;

Energy destruction, $I_{exp} = m(\psi_4 - \psi_3) = m(s_4 - s_3)[Throttling, h_4 = h_1]$ (2.11)

Coefficient of performance; $COP = \frac{Q_{ev}}{W_{el}}$ (2.12)

Total destruction; $I_{total} = I_{cond} + I_{exp} + I_{comp} + I_{evap}$ (2.13)

Exergy efficiency; $\eta_x = \frac{\psi_1 - \psi_4}{W_{el}}$ (2.14)

Energy efficiency ratio; $EER = \frac{Energy\ out}{Work\ of\ Compression} = \frac{h_1 - h_4}{W_{el}}$ (2.15)

3. MODEL DESCRIPTION

The general structure of the proposed model is presented in Fig. 3.2., where it can be seen that the model inputs are the secondary fluids/nanofluid input variables and the compressor speed, neglecting sub-cooling degree at the condenser outlet and superheating degree at the evaporator outlet, for simplicity. Using these inputs and the main characteristics of the compressor and heat exchangers, the model predicts the operating pressures (without considering pressure drops), secondary fluids output variables and the energy performance. Flow of refrigerant in both condenser & evaporator is counter flow. In the evaporator, refrigerant flows inside the inner tube; nanofluid surrounding the inner tube and the condenser water flows inside the inner tube and refrigerant surrounding the inner tube. The model computes the refrigerant properties and the thermo-physical properties of secondary fluids are evaluated by using Engineering equation solver *(EES)*. The model consists of a set of five equations based on physical laws describing the main parts of the system, as shown schematically in the figure below. The refrigerant states are numbered; the refrigerant mass flow rate *(mr)* has been modeled using Eq. (16), where the compressor volumetric efficiency (ηv) has been expressed as a function of operating pressure and compressor speed (*N)* as shown in Eq. (17). For simplicity, *(ρ1)* is the refrigerant density considered is the one corresponding to the saturated vapor at the evaporating pressure and *Vg* is the geometric compressor volume.

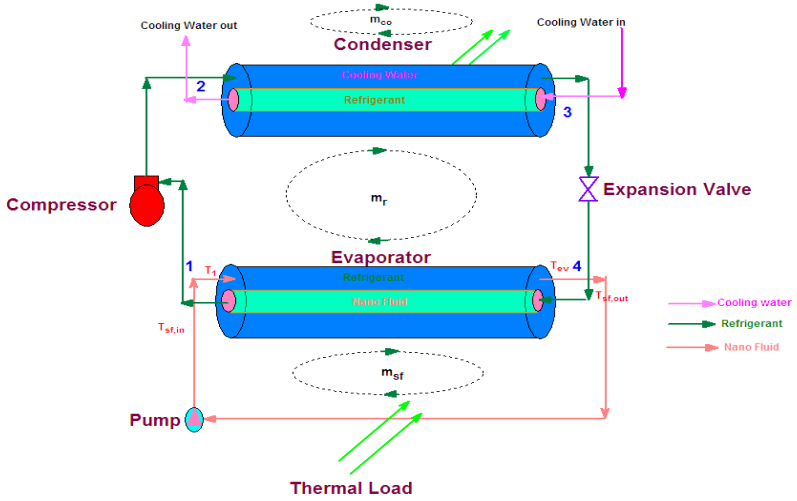

Fig. 2: Schematic structure of model

The model consists of a set of five equations based on physical laws describing the main parts of the system, as shown schematically in Fig. 2.1 The refrigerant states are numbered in Fig. 2.2. The refrigerant mass flow rate *(mr)* has been modeled using Eq. (1), where the compressor volumetric efficiency (ηv) has been expressed as a function of operating pressure and compressor speed (*N)* as shown in Eq. (2). For simplicity, *(ρ1)* is the refrigerant density considered is the one corresponding to the saturated vapor at the evaporating pressure and *Vg* is the geometric compressor volume.

$$Mr = n_v . \rho_1 . V_g . N \quad (2.16)$$

$$n_v = 0.73341 - 0.00003062 \cdot N + 0.04561 \cdot P_e - 0.01237 \cdot P_k \quad (2.17)$$

Where, P_k & P_e is the condenser and evaporator pressure respectively.

3.1 Evaporator Formulation

The evaporator is modeled using two equations, one based on the heat exchanger energy balance,

$$m_r . (h_1 - h_5) = m_b . Cpb . (Tb_{in} - Tb_{out}) \quad (2.18)$$

Where, h_1 and h_5 is the enthalpy at state 1 and 5 of refrigerant, *Cpb* is the Specific heat of brine. Tb_{in} and Tb_{out} is the inlet and outlet Temperature of the brine

.The other making use of the logarithmic mean temperature difference and the global heat transfer coefficient, with a LMTD correction factor equal to 1

$$m_r . (h_1 - h_5) = u_e - S_e . \left(\frac{Tb_{in} - T_e - (Tb_{out} - T_e)}{In \frac{Tb_{in} - T_e}{Tb_{out} - T_e}} \right) \quad (2.19)$$

Where, *Ue*is the evaporator global heat transfer. *Se* is the surface area of the evaporator. *Te* is the evaporator Temperature. The evaporator global heat transfer coefficient *(Ue)* used in Eq. *(2.20)* is computed as:

$$U_e = \frac{1}{r_0} . \left(\frac{1}{a_b . r_0} + \frac{ln \frac{r_0}{r_1}}{K_m} + \frac{1}{a_{iv} . r_i} + R_{F0} \right)^{-1} \quad (2.20)$$

Where,

KM is the thermal conductivity of Metal.

r_i & r_o is the outside and inside radius of the tube respectively.

α_{iv} is the heat transfer coefficient for the refrigerant.

RT_{Fo} is the thermal resistance associated to the fouling in the heat exchanger tubes (RT_{Fo} = 0.000086 m2 K/W, manufacturer data for water/water).

The heat transfer coefficient for the brine *(αb)* is computed using the Zukauskas' correlation.

$$a_b = \frac{K_b}{D_o} . C_1 . Re_b^{m1} . Pr_b^{0.36} . \left(\frac{\mu_b}{\mu_{bM}} \right)^{0.25} \quad (2.21)$$

Where,

Kb is the thermal conductivity of brine.

D_O is the outer diameter of tube.

R_{eb} is the Reynold's No. of brine.

P_{rb} is the Prandle No. of brine.

C_1 and m_1 is a coefficient of the correlation.

μbviscosity of brine.

μbM viscosity of brine at metal temperature.

While the refrigerant heat transfer coefficient *(αlv)* is computed With the Chen's correlation.

$$\propto_{IV} = sf.\propto_{nb} + F.\propto_{conv} \quad (2.22)$$

Where,

α_{nb} is the nucleated boiling component obtained using Foster– Zuber correlation.

α_{conv} is the convective component, computed using the Dittus– Boelter correlation.

sf is the suppression factor.

F is the Reynolds number factor.

The values of these parameters are computed using the following equations:

$$\propto_{nb} = 0.00122.\frac{K_{Le}^{0.79}.Cp_{Le}^{0.45}.\rho_{Le}^{0.49}}{\sigma^{0.79}.\mu_{Le}^{0.29}.\lambda_e^{0.24}.\rho_{ve}^{0.24}}.\delta T_{sat}^{0.24}.\delta P_{sat}^{0.75} \quad (2.23)$$

Where,

σ is the surface tension of refrigerant.

K_{Le} is the thermal conductivity of refrigerant in liquid phase in evaporator.

Cp_{Le} is the specific heat of refrigerant in liquid phase in evaporator.

ρve & ρLe is the density of refrigerant in vapor and liquid phase in evaporator.

$\lambda\, e$ is the latent heat in evaporator.

$$\propto_{conv} = 0.023.R_e^{0.8}.P_r^{0.4}.\frac{K_L}{D_i} \quad (2.24)$$

$$sf = \frac{1}{(1+0.00000253).(Re.F^{1.15})^{1.17}} \quad (2.25)$$

$$F = \begin{Bmatrix} 1, & 1/Xtt < 0.1 \\ 2.35\,(1/Xtt + 0.213)^{0.736}, & 1/Xtt < 0.1 \end{Bmatrix} \quad (2.26)$$

Where,

Di is the coil inner diameter.

Xtt is the Martinelli's Parameter.

Xv is the quality of refrigerant.

$$Xtt = \left[\frac{1-Xv}{Xv}\right]^{0.9}.\left[\frac{\rho v}{\rho l}\right]^{0.9}.\left[\frac{\mu L}{\mu v}\right]^{0.1} \quad (2.27)$$

3.2 Compressor Formulation

The compressor behavior is modeled from the isentropic efficiency *(η_{is})* and the working pressures. Thus, from the refrigerant state at the evaporator outlet, the refrigerant state at the compressor discharge is determined using Eq. *(28)* from the isentropic compression work and the compression isentropic efficiency,

$$h_2 = h_1 + \frac{h_{2s} - h_1}{\eta_{is}} \quad (2.28)$$

Where, η_{is} is the compression isentropic efficiency and it has been obtained from gathered empirical data, as a function of operating pressures, yielding Eq. *(29):*

$$\eta_{is} = 0.156323 + 0.0000912 \cdot N + 0.004302 \cdot Pk + 0.09151 \cdot Pe \quad (2.29)$$

In order to compute the compressor power consumption, the model makes use of a global electromechanical efficiency fitted with the empirical data as a function of *N*,

$$\eta_g = 0.00002805 \cdot N^2 + 0.02593961 \cdot N + 6.4965 \quad (2.30)$$

As in the case of Eq.(17) the efficiencies given by Eq. (29) and (30) Show a significant relationship among the variables with a confidence level of 99%. The correlations for isentropic and electromechanical efficiency are fitted for the compressor used in the facility, and similar relations should be obtained from experimental results for another compressor. The heat transfer from the refrigerant at the compressor discharge line to the condenser inlet has been modeled, due to the considerable length of the line in the experimental chiller facility, using expression (2.28)

$$m_r.(h_2 - h_3) = \mu_{23} - S_{23}.\left(\frac{T_2 - T_{air} - (T_s - T_{air})}{In\left(\frac{T_2 - T_{air}}{T_s - T_{air}}\right)}\right) \quad (2.31)$$

μ_{23} is the global heat transfer coefficient used in Eq. (26) is computed as:

$$\mu_{23} = \frac{1}{r_o}.\left(\frac{1}{\propto_i - r_i} + \frac{In\left(\frac{r_o}{r_i}\right)}{K_M} + \frac{1}{\propto_o - r_o}\right)^{-1} \quad (2.32)$$

Using a modified version of the Gnielinski's correlation (33a) for the refrigerant inside the tubes, *αi*.

If Re < 10000 then use,

$$\propto_1 = \frac{Kv}{2 - r_i}.\left[\frac{\frac{Fric}{8}.(Re - 1000).Pr}{1 + 12.7.\left(\frac{Fric}{8}\right)^{0.5}.(Pr^{2/3} - 1)}\right].\left[\frac{\mu_v}{\mu_v M}\right]^{0.11} \quad (2.33a)$$

Or, If Re >10000 then use,

$$\propto_1 = \left[\frac{Kv}{2 - r_i}\right]^{0.027}.Re^{(4/5)}.Pr^{(1/3)}.\left[\frac{\mu_v}{\mu_v M}\right]^{0.14} \quad (2.33b)$$

Where,

$$Fric = \frac{1}{(0.79\,In(Re) - 1.64)^2} \quad (2.34)$$

and the natural-convection heat transfer coefficient is computed as,

$$\propto_o = \frac{K_{air}}{D_o}.(Nul^{10} + Nutt^{10})^{\left[\frac{1}{10}\right]} \quad (2.35)$$

Where,

$$Nul = 2.\frac{fc}{In\left[1 + \frac{2.fc}{NuT}\right]} \quad (2.36)$$

$$Nutt = 0.103.Ra^{1/3} \quad (2.37)$$

Being,

$$NuT = 0.7772 * 0.103 * Ra^{0.25} \quad (2.38)$$

$$F = 1 - \frac{0.13}{NuT^{0.16}} \quad (2.39)$$

$$Ra = g.\frac{1}{T_{air}}.(T_M - T_{air}).\frac{(2.r_o)^3}{\frac{\mu_{air} - K_{air}}{\rho_{air}\,\rho_{air}\,CP_{air}}} \quad (2.40)$$

3.3 Condenser Formulation

The condenser behavior is modeled by dividing the heat exchanger into two zones: the superheated vapor zone and the condensing zone, assuming no sub-cooling at the condenser outlet, as it has been stated in the assumptions. The overall heat exchanger is then modeled with two energy balances, one using the secondary fluid heat flow rate.

And the other making use of the global heat transfer coefficient and assuming a LMTD correction factor equal to 1 for simplicity,

$$m_r.(h_3 - h_{vsat}) = m_w.Cp_w.(Tw_{out} - Tw_m) \quad (2.41)$$

$$M_r.(h_3 - h_{vsat}) = U_v.S_v.\left[\frac{T_k - TW_m - (T_s - TW_{out})}{In\left(\frac{T_k - TW_m}{T_s - TW_{out}}\right)}\right] \quad (2.42)$$

Being *UK* an average heat transfer coefficient computed as,

$$U_k = \frac{U_v.S_v + U_{vl}.(S_k - S_v)}{S_k} \quad (2.43)$$

Where,

SK is the overall heat transfer area of the heat exchanger.

SV is the theoretical heat transfer area dedicated to the superheated vapor zone.

$$\text{Sv L} = S_k - \text{Sv} \quad (2.44)$$

$$M_r.(h_{vsat} - h_{Lsat}) = U_{vl}.S_{vl}.\left[\frac{T_k - TW_m - (T_k - TW_n)}{In\left(\frac{T_k - TW_m}{T_k - TW_n}\right)}\right] \quad (2.45)$$

In the calculation of the partial heat transfer coefficients, *UV* and *UVL*, the convection heat transfer coefficient in the water side is computed. For the computation of the convection heat transfer coefficient associated to the refrigerant one can distinguish between the convection heat transfer coefficient in the superheated vapor zone, given by,

$$\alpha_v = \frac{K_v}{D_o}.C_1.Re^{m_1}.Pr^{0.36}.\left[\frac{\mu_v}{\mu_{vM}}\right]^{0.25} \quad (2.46)$$

Where, *C1* and *m1* depend on the Reynolds number value,

$$[C_1, m_1] = \begin{cases} [0.9, 0.4] & Re \le 100 \\ [0.683, 0.466] & 100 < Re \le 1000 \\ [0.4, 0.6] & 1000 < Re \le 200000 \\ [0.022, 0.84] & Re > 200000 \end{cases} \quad (2.47)$$

and the convection heat transfer coefficient in the condensing zone, that is computed as,

$$\alpha_k = 0.729.\left[\frac{g.\rho_L.(\rho_L - \rho_v).\lambda_{k,mod}.K_l^3}{\mu_l.T_{abs}.2.r_o}\right]^{0.25} \quad (2.48)$$

Being λKmod the modified latent heat with the effects of thermal advection

$$\lambda_{k,mod} = \lambda_k.(1 + 0.68.j_a) \quad (2.49)$$

Where,

$$\lambda_k = h_3 - h_{vsat} \quad (2.50)$$

and *Ja* is the Jacobsen's number.

$$J_a - \frac{CP_L.T_{abs}}{\lambda_k} \quad (2.51)$$

And

$$T_{abs} = T_k - T_M \quad (2.52)$$

3.4. Nanofluids

The nanofluid is treated as a homogeneous fluid. Based on experimental data of several authors, [7] the following correlation for was proposed the thermal conductivity of nanofluids:

$$\frac{K_{nf}}{K_m} = cRe_m^{0.175}\emptyset_p^{0.05}\left(\frac{K_p}{K_m}\right)^{0.2324} \quad (2.53)$$

Where K_{nf} is the thermal conductivity of nanofluid, $K_m$is the thermal conductivity of refrigerant,K_p is the thermal conductivity of nanoparticles, c is constant in the equation, $\emptyset_p$ is the particle volume fraction, V_m is the velocity of the refrigerant, ρ_p is the density of nanoparticles, d_p is the diameter of nanoparticles, and T_{in} is the temperature inlet. The Reynolds number of nanorefrigerant is calculated by using:

$$Re_m = \left(\frac{1}{V_m}\right)\left(\frac{18K_pT_{in}}{\pi\rho_p d_p}\right)^{\frac{1}{2}} \quad (2.54)$$

Mahbubul et al. [8] introduced the Brinkman formula to determine the viscosity of nanorefrigerant, which has been used to determine the nanofluids' viscosity:

$$\mu_{r,n,L} = \mu_{r,L}\frac{1}{(1-\emptyset)^{2.5}} \quad (2.55)$$

Finally, density and specific heat are determined based on mass and energy balances, respectively.

$$\rho_{nf} = \rho_p\emptyset_p + \rho_m(1-\emptyset_p) \quad (2.56)$$

Where ρ_m is the density of the refrigerant

$$c_{p,nf} = \frac{\emptyset_p\rho_p c_{p,p}+(1-\emptyset_p)\rho_f c_{p,f}}{\rho_{nf}} \quad (2.57)$$

Pressure drop on the nanofluid side was calculated in the same way as for any other fluid

[9].

Volume fraction of nanofluid

$$\rho_p = \frac{\omega_n\rho_m}{(\omega_n\rho_m+(1-\omega_n)\emptyset_p)} \quad (2.58)$$

Where $\omega_n = mass\ fraction = \frac{M_p}{M_p+M_m}$ (2.59)

4. RESULTS AND DISCUSSION

Input data for the thermal modeling included the geometry of compressor and heat exchangers (inner and outer diameters), HFC-134A and HFO-1234YF refrigerant properties, Copper oxide nanofluid properties characteristics (base fluid and nanoparticle material, size and volume fraction), inlet temperatures of condenser coolant (Water) and secondary fluid (nanofluid), condensing and evaporating temperatures. The resulting system of equations was solved using the EES (Engineering Equation Solver) software.

Table 4: Variations of performance parameters with evaporating temperature in the vapour compression refrigerating system using HFC–134a mixed with copper oxide nanoparticles of 10 micron particles diameter and 5% volume fraction.

Evaporating Temperature (ºC)	C. O. P	Exergy Efficiency	E. D. R
-40	1.65	0.163	2.75
-30	2.05	0.205	2.95
-20	2.06	0.259	3.64
-10	3.42	0.272	4.84

Table 5: Variations of performance parameters with degree of sub-cooling in the vapour compression refrigerating system using HFC–134a mixed with copper oxide nanoparticles of 10 micron particles diameter and 5% volume fraction.

Degree of sub-cooling (ºC)	C. O. P	Exergy Efficiency	E. D. R
0	3.22	0.193	4.17
3	3.31	0.201	3.97
5	3.42	0.204	3.89
7	3.48	0.209	3.81
10	3.57	0.214	3.68

Table 6: Variations of performance parameters with evaporating temperature in the vapour compression refrigerating system using HFO–1234yf mixed with copper oxide nanoparticles of 10 micron particles diameter and 5% volume fraction.

Evaporating Temperature (ºC)	C. O. P	Exergy Efficiency	E. D. R
-40	1.55	0.121	3.23
-30	1.96	0.163	3.41
-20	2.47	0.912	3.98
-10	3.34	0.207	4.93

Table 7: Variations of performance parameters with degree of sub-cooling in the vapour compression refrigerating system using HFC–1234yf mixed with copper oxide nanoparticles of 10 micron particles diameter and 5% volume fraction.

Degree of sub-cooling (ºC)	C. O. P	Exergy Efficiency	E. D. R
0	3.16	0.187	4.42
3	3.20	0.192	4.34
5	3.33	0.197	4.21
7	3.39	0.201	4.12
10	3.50	0.204	3.98

Simulation main results include: (i) Effect of evaporating temperature on Coefficient of performance (ii) Effect of degree of sub-cooling on Coefficient of performance (iii) Effect of evaporating temperature on Exergy efficient. (iv) Effect of evaporating temperature on Exergy Destruction Rate (v) Effect of Degree of sub-cooling on exergy efficiency. (vi) Effect of degree of sub-cooling on exergy destruction rate.

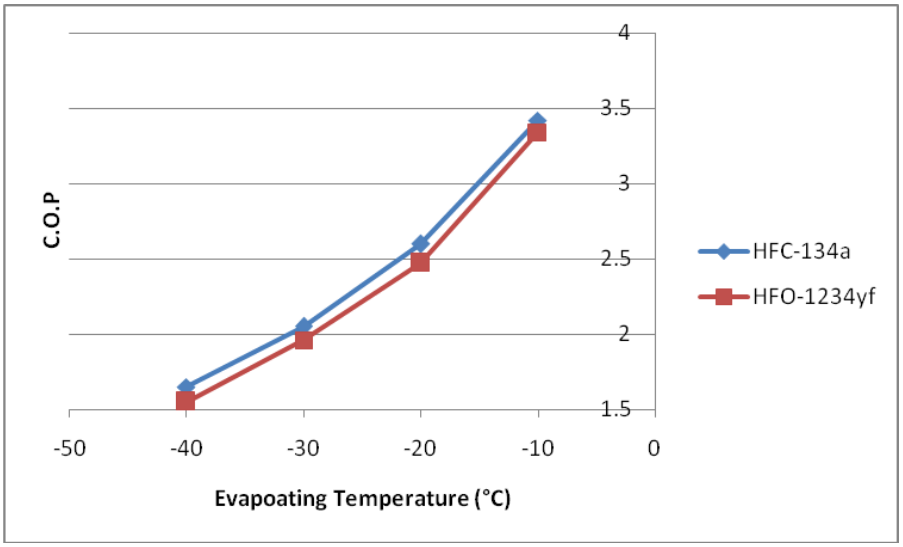

Fig 3: Variation of C.O.P with Evaporating Temperature (°C)

Figure 3 shows the effect of evaporating temperature on Coefficient of Performance; with increase in evaporator temperature, the pressure ratio across the compressor decreases, causing work done by the compressor decrease and cooling capacity increases due to increase in refrigerating effect. Hence, the combined effect of these two factors increases the COP of the vapour compression refrigeration system. HFC-134a mixed with CuO nanoparticle shows better C.O.P than HFO-1234yf mixed with CuO nanoparticle with increase in evaporating temperature.

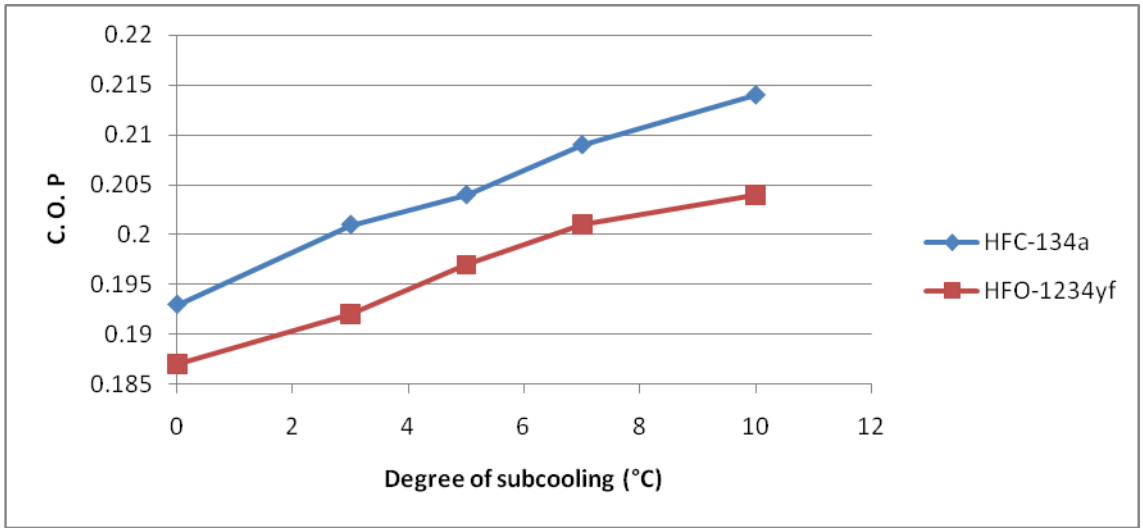

Fig 4: Variation of C.O.P with Degree of Sub-cooling (°C)

Figure 4 shows the variation of C.O.P with sub-cooling of liquid refrigerant at the exit of condenser. It is evident that increase in degree of sub-cooling increases the cooling capacity because of increase in refrigerating effect and there is no change in compressor work, hence COP increases. HFO-1234yf mixed with CuO nanoparticle shows better C.O.P than HFC-134a mixed with CuO nanoparticle with increase in degree of subcooling.

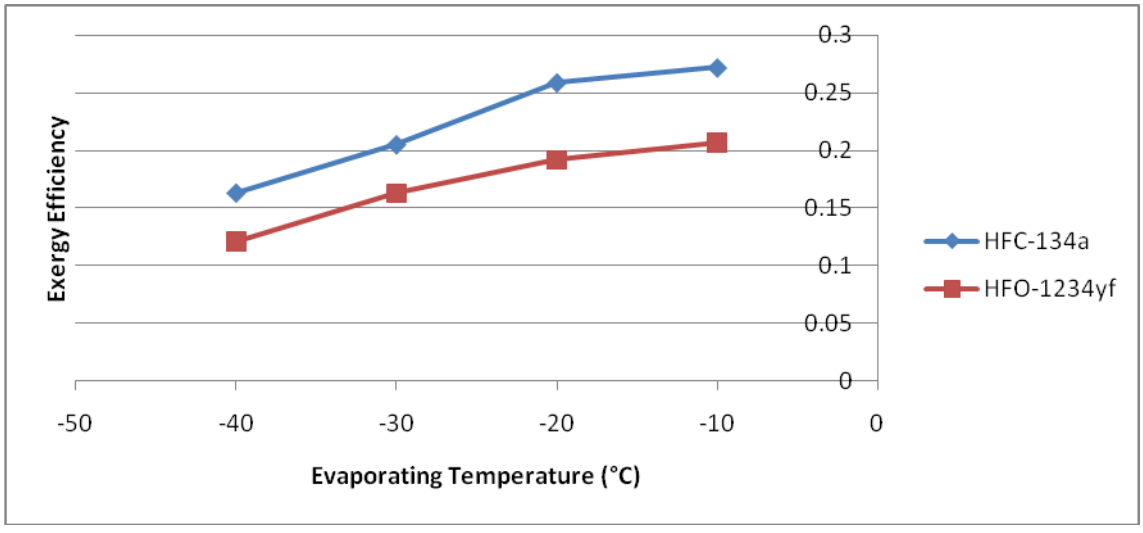

Fig 5: Variation of Exergy Efficiency with Evaporating Temperature (°C)

Figures 5 show the effect of evaporator temperatures on exergetic efficiency; with increase in evaporator temperatures exergetic efficiency decreases. The optimum evaporator is the temperature at which maximum exergetic efficiency is obtained. HFC-134a with CuO nanoparticles has the highest exergy efficiency.

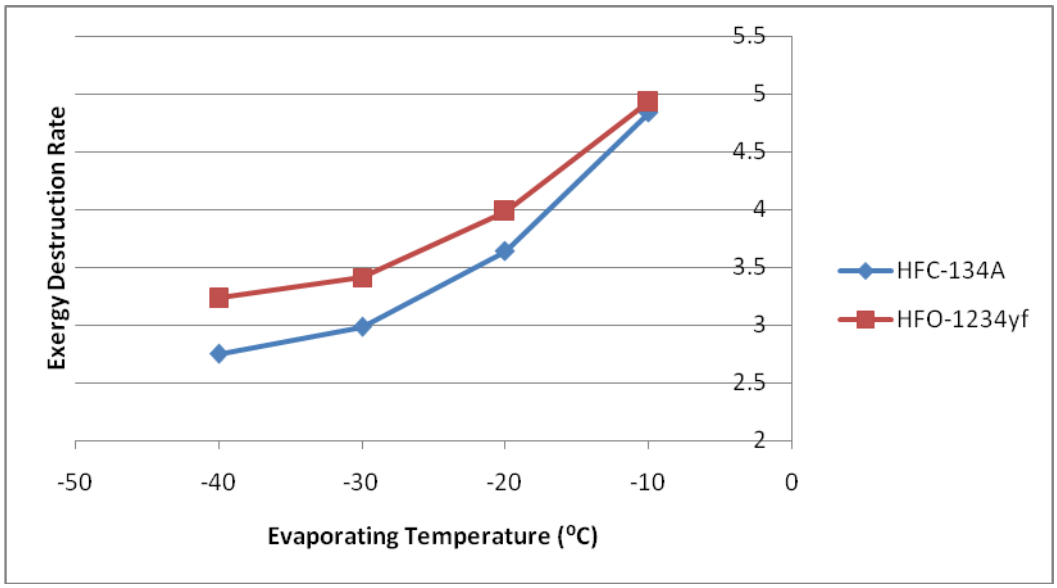

Fig 6: Variation of Exergy Destruction Rate with Evaporating Temperature (°C)

Figure 6 represents the curves trend for EDR almost reverses to curves of exergetic efficiency. The rise and fall of the exergetic efficiency, depends upon the two parameters. First parameter is the exergy of cooling effects, i.e. $Qe\left(1-\frac{T_o}{T_r}\right)$ with increase in evaporator temperature Qe increases whereas the term $\left(1-\frac{T_o}{T_r}\right)$reduces. Second parameter is the compressor work required by compressor W which decreases with increase in evaporator temperature. Both terms Qe and W have positive effect on increase of exergetic efficiency whereas the term $\left(1-\frac{T_o}{T_r}\right)$ has negative effect on increase of exergetic efficiency. The combined effects of these two parameters, increases exergetic efficiency till the optimum evaporator temperature and beyond the optimum temperature decrease. Because of exergetic efficiency is inversely proportional to EDR; the curves trend for EDR almost reverses to curves of exergetic efficiency. With increases in evaporating temperatures, EDR decreases till the optimum evaporator temperature and beyond this optimum temperature it increase. The optimum evaporator is the temperature at which minimum EDR is obtained. It has been observed that trend shown by curves of EDR is reverse of that shown by curves of exergetic efficiency EDR of HFO-1234yf with CuO nanoparticle is higher than HFC-134a with CuO nanoparticle and this difference decreases in the range 5.8-18.8% as the evaporator temperature increases.

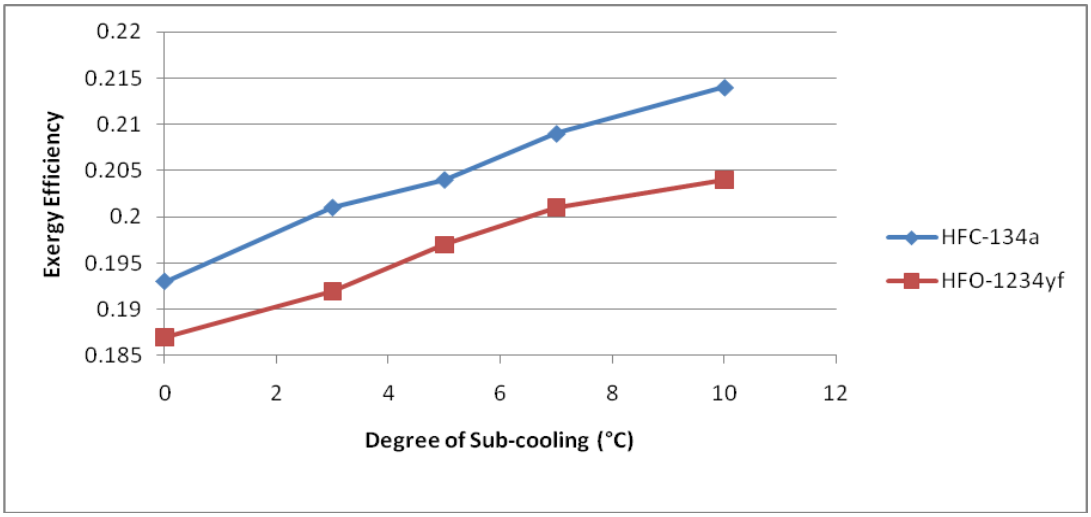

Fig 7: Variation of Exergy Efficiency with Degree of Sub-cooling (°C)

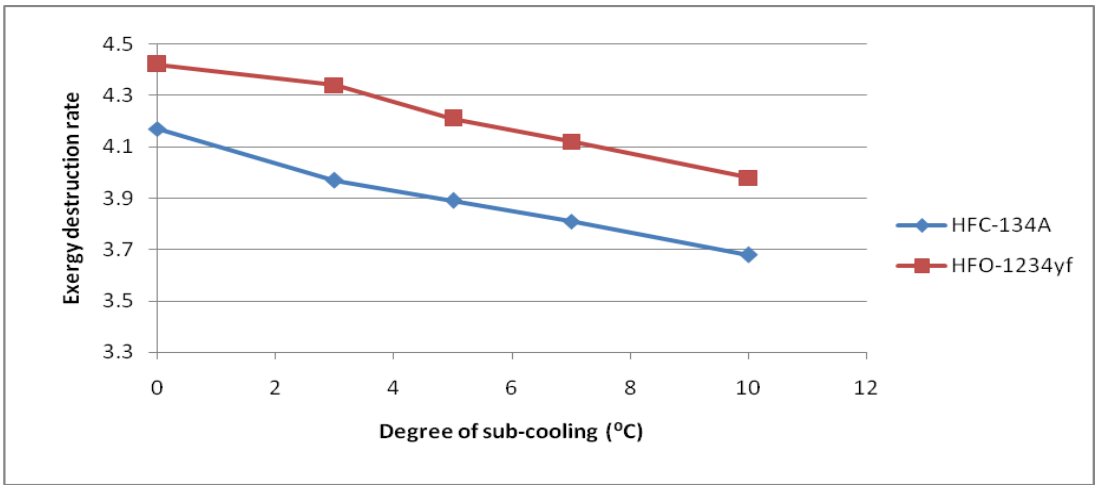

Fig 8: Variation of Exergy Destruction Rate with Degree of Sub-cooling (°C)

Figures 7 and 8 presents the effect of degree of sub-cooling on exergetic efficiency and EDR; It is evident that increase in degree of sub-cooling increases the cooling capacity because of increase in refrigerating effect and there is no change in compressor work, hence COP increases. From the study, it is evident that increase in COP increases the exergetic efficiency and reduces the EDR. HFC-134a has the highest exergy efficiency on different ranges of sub-cooling which are 0.193, 0.201, 0.204, 0.209 & 0.214 0n 0°C, 3°C, 5°C, 7°C & 10°C except on sub-cooling which HFO-1234YF has maximum E.D.R than HFC-134A.

Table: 8: Performance evaluations (% Improvements in first law efficiency) of vapour compression refrigeration system using HFC-134a and HFO-1234yf refrigerant in the primary circuit and 5% volume fraction of CuO nanoparticle of 10 micron size in the secondary circuit in the evaporator.

Refrigerant	C.O.P with CuO nano	C.O.P without nano	% improvement
HFC-134a	3.224	2.812	14.65%
HFO-1234yf	3.051	2.704	12.83%

Table: 9: Performance evaluations (% Improvements in exergy efficiency) of vapour compression refrigeration system using HFC-134a and HFO-1234yf refrigerant in the primary circuit and 5% volume fraction of CuO nanoparticle of 10 micron size in the secondary circuit in the evaporator.

Refrigerant	Exergy efficiency with CuO nano	Exergy efficiency without nano	% improvement
HFC-134a	0.376	0.233	12.9%
HFO-1234yf	0.359	0.322	11.67%

Table: 10: Performance evaluations (% Improvements in exergy destruction ratio (E.D.R)) of vapour compression refrigeration system using HFC-134a and HFO-1234yf refrigerant in the primary circuit and 5% volume fraction of CuO nanoparticle of 10 micron size in the secondary circuit in the evaporator.

Refrigerant	E.D.R with CuO nano	E.D.R without nano	% improvement
HFC-134a	2.952	3.673	20.2%
HFO-1234yf	3.411	4.188	18.84%

5. CONCLUSIONS

This research paper presents the modeling of vapor compression refrigeration system based on brine cooled evaporating temperature and degree of subcooling using ecofriendly refrigerants. Thus, vapour compression refrigeration which will work on environment friendly refrigerants can be modeled conveniently using above model. Exergy analysis is performed on the above system‘s experimental setup.

The following conclusions are drawn from the energy and exergy analysis based on evaporating temperature and sub-cooling.

- As evaporator temperature increases, the first law energy performance and second law efficiency increases.
- Results obtained shows that the highest improved C.O.P is 14.65% in HFC-134a mixed with nanoparticles as compared to without nanoparticles.
- It was also observed that second law performance improvement of exergy efficiency is 11.6% to 12.9% and it's higher in HFC-134a/CuO nano mixture.
- The reduction in the irreversibility in terms of exergy destruction ratio in the system is 21.4% using the HFC-134a/CuO nano mixture and 18.5% using the HFO-1234yf/CuO nano mixture.
- Finally, the mixture of CuO nano in HFC-134a shows a higher performance in most cases of the vapor compression refrigeration system.

REFERENCES

[1] Ahamed J.U., Saidur R., Masjuki H.H. (2011) "A review on exergy analysis of vapor compression refrigeration system" *Int J Renewable and sustainable energy reviews.2011; 15:1593-1600.*

[2] Ahmad H. Sabry and Pin Jern Ker, (2021). Improvement on energy consumption of a refrigerator within PV system including battery storage. *Energy Reports, Volume 7, November 2021, Pages 4430-438.*

[3] Azimi, M and.Mozaffari, A. (2015). Heat Transfer and Transfer analysis of unsteady grapheme Oxide nanofluid flow using a fuzzy identifier evolved by genetically encoded mutable smart bee algorithm. *Engineering science and Technology, an International Journal 18(1), 106-123, 2015*

[4] Mahmood Mustani, Joybari, Mohammad Sadegh Hatamipour, Amir Rahimi, (2013) "Exergy analysis and optimization of R600a as a replacement of R134a in a domestic refrigerator system. *International Journal of refrigeration; Vol-36, pp.1233-1242.*

[5] Sahim et al. (2005). Supplementation of zinc from organic or inorganic.

[6] Bayrakci et al. (2009). Energy and Exergy analysis of Vapour Compression refrigeration system using pure hydrocarbon refrigerants. *International journal of Energy Research 33(12), 1070-10775, 2009.*

[7] Velagapudi et al. (2009).

[8] Mahbubul et al. (2013). Thermophysical properties and heat transfer performance of AL2O3/ R-134a Nanorefrigerants. *Internationl Journal of Heat and Mass transfer 57 (1) 100-108.*

[9] Xuan, Y., & Li, Q. (2003). Investigation on Convective Heat Transfer and Flow Features of Nanofluids. *Journal of Heat Transfer, 125*, 150 - 152.